Experimental Measurements of the Ionization Coefficient (β) for Silicon and Iron Micrometeoroids During Ablation in Air and N_2

Santiago Pinzón-Cortés[1,2], Austin Smith[3], Juan Diego Carrillo-Sanchez[1,2], Zoltan Sternovsky[3], Diego Janches[2]

1. NASA/Goddard Space Flight Center 2. Department of Physics, Catholic University of America. 3. LASP/ CU Boulder

Abstract

In this work, we used University of Colorado facilities to calculate new experimental values of β for Si and to expand existing measurements for Fe. Additionally, we reanalyzed existing experimental data for Al. Si particles were accelerated to velocities between 10 and 50 km/s in air and N_2, while Fe particles were accelerated between 8 to 20 km/s. The data obtained were compared with previous models and previous experimental measurements. These new measurements improve the accuracy of β models and provide a better understanding of the ablation process. These results will improve the radar detection models and enhance the characterization of micrometeorids entering Earth's atmosphere.

Introduction

A key parameter in the ablation process is the ionization coefficient, β. This parameter characterizes the ionization produced during meteoroid-atmosphere collisions. β can be used to estimate meteoroid mass, flux, density and height distribution from radar observations. Studies made with radar observations assumed that the composition of most meteoroids is chondritic [4]. This implies that the principal elements that constitute a meteoroid are Fe, Mg, Si, O and C. Laboratory measurements of β for those elements, particularly at low velocity conditions (10 - 20 km/s) are needed to improve model accuracy. Improved β values will help reconcile the discrepancy between radar-detected meteoroid fluxes and theoretical model predictions [2].

Methodology

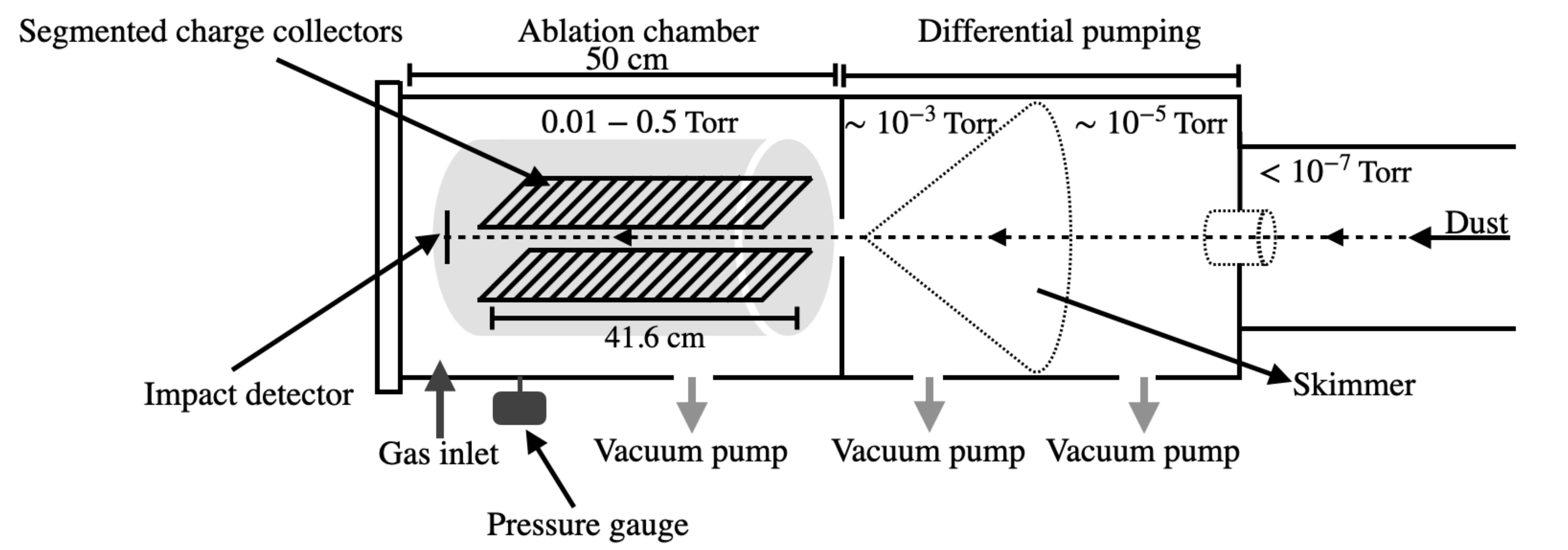

Figure 1. The open access ablation facility operated at the University of Colorado. (Image not to scale)

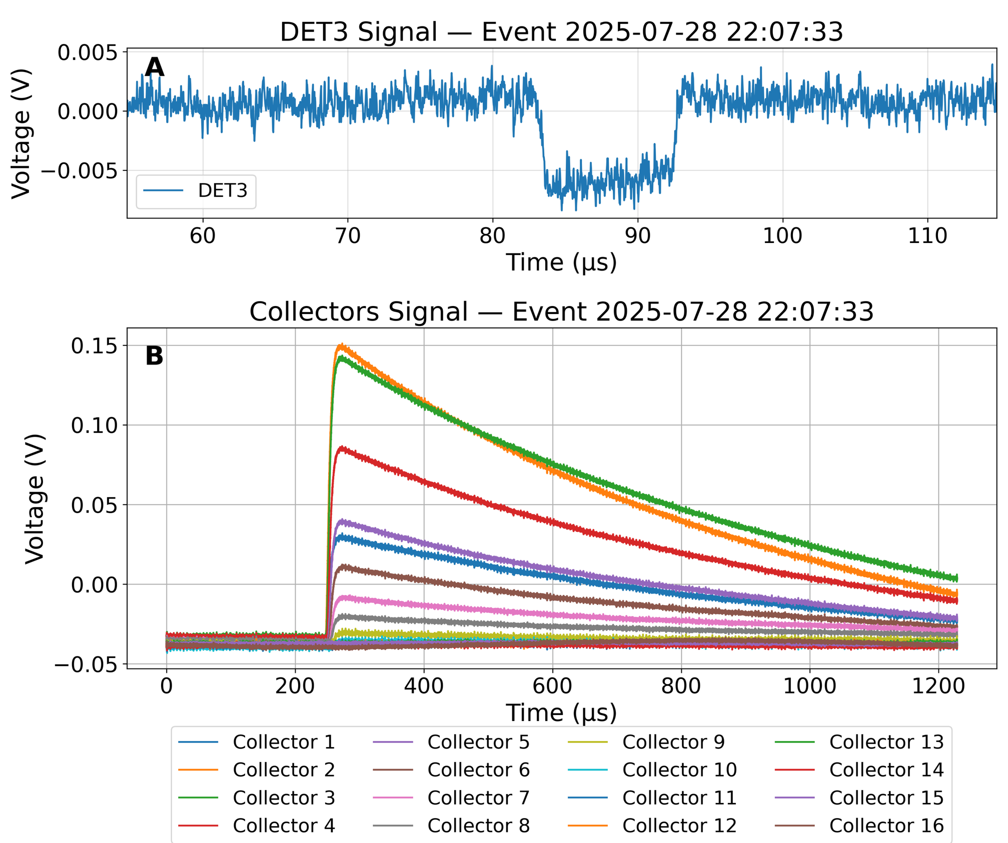

Figure 2. A) Example of the DET3 signal. B) Example of the signal obtained from the 16 charge collectors.

Voltage drop is used to calculate initial velocity (v) and initial charge (Q) from horizontal and vertical difference respectively

$$m = \frac{2QU}{v^2}$$

U = accelerator voltage

$$\beta_{exp} = \frac{M \sum_{i=1}^{16} q_i}{em} \quad \text{(Eq 1)}$$

M = Molecular mass

e = electron charge

Jones (1997) Model

$$\beta(v) = \beta_0(v) + (1 - \beta_0(v))\frac{(1+\mu)^2}{2v^2\mu}\int_{v0}^{v} \beta(v')v'dv' \quad \text{(Eq 2)}$$

$$\beta_0(v) = \frac{c(v-v_0)^2 v^{0.8}}{1 + c(v-v_0)^2 v^{0.8}}$$

$$v_{0,i} = \sqrt{\frac{2(M_i + M_{gas})E_i}{M_i M_{gas}}}$$

Deluca et al. (2018) Model

$$\beta(v) = \frac{c(v-v_0)^n v^{0.8}}{1 + c(v-v_0)^n v^{0.8}} \quad \text{(Eq 3)}$$

Janches et al. (2017)

$$c(X) = c(Fe) \times \left(\frac{\psi(Fe)}{\psi(X)}\right)^2 \quad \text{(Eq 4)}$$

1. We made measurements of the ionization coefficient using the Dust Accelerator at the University of Colorado (Fig. 1).
2. β was obtained for Si in N_2 and Air, and new β measurements for Fe in Air were collected using Eq 1.
3. The empirical models (Eq. 2 and Eq. 3) were fitted to the data using a weighted iterative method to obtain the best fit parameters c and n.
4. A two-regime Binned fitting approach was proposed to better represent $\beta(v)$ across the full velocity range for Fe, Si and Al.

Results and Discussion

Table 1. Threshold velocity (v_0), fitted parameters c and n for the ionization coefficient model for Fe and Si in air reported in previous studies. († Units of c are $(s/km)^{2.8}$. ‡ Units of c are $(s/km)^{2.4}$)

Element	Gas	v_0 (km/s)	Source	c	n
Fe	Air	8.95	Jones (1997)	$3.45 \times 10^{-5\dagger}$	2.0
			Thomas et al. (2016)	$1.97 \times 10^{-5\dagger}$	2.0
			Janches et al. (2017)	$1.97 \times 10^{-5\dagger}$	2.0
			DeLuca et al. (2018)	$(1.95 \pm 0.03) \times 10^{-4\ddagger}$	1.6 (fixed)
Al	Air	9.10	DeLuca et al. (2018)	$1.60 \times 10^{-4\ddagger}$	1.6 (fixed)
Si	Air	10.51	Jones (1997)	$1.85 \times 10^{-5\dagger}$	2.0
			Janches et al. (2017)	$1.85 \times 10^{-5\dagger}$	2.0

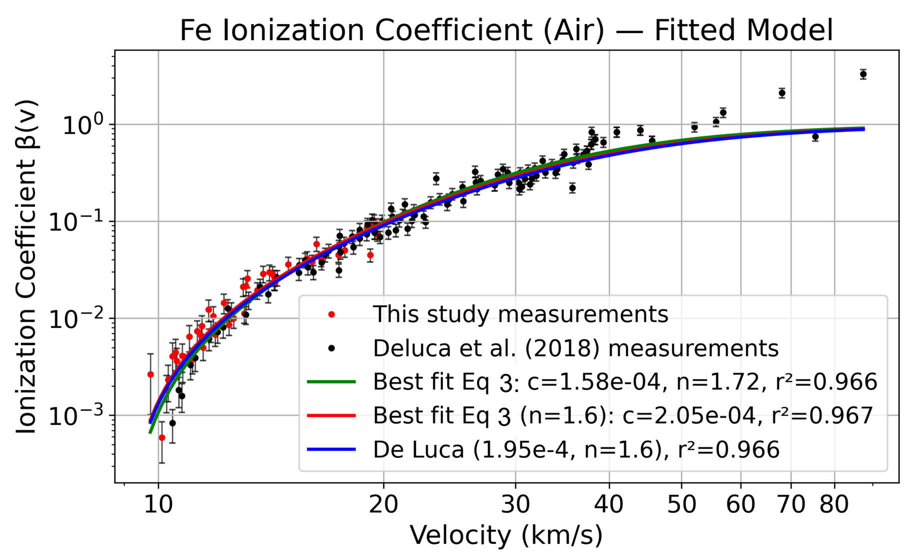

Figure 3. β measurements for Fe in Air as a function of velocity.

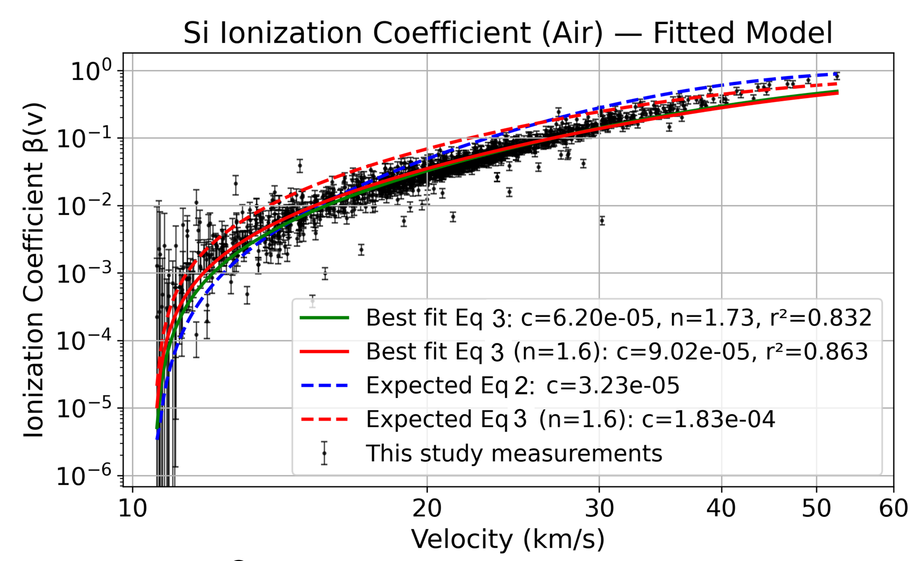

Figure 4. β measurements for Si in Air as a function of velocity.

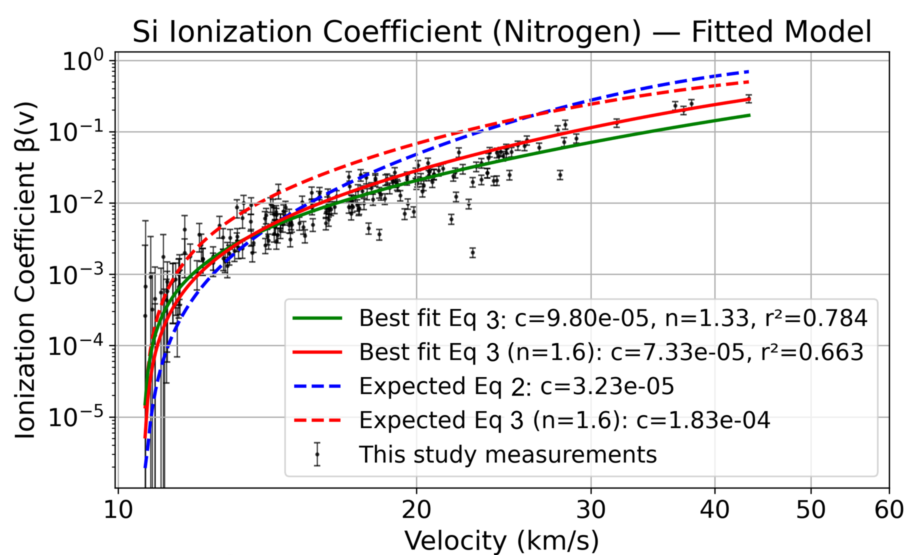

Figure 5. β measurements for Si in N_2 as a function of velocity.

- The expected models consistently deviate across the full velocity range (Figs. 4–5): Eq. 2 underestimates at low velocities and overestimates at high velocities, while Eq. 3 overestimates in the whole range of velocities
- Fitted models also show systematic deviations (Figs. 3–5): fixing n = 1.6 in Eq. 3 underestimates high velocity measurements, while allowing both c and n to vary underestimates across low and high velocity regimes

Since no single model can explain the full velocity range, we propose a two-regime approach dividing the data into a low velocity regime ($v \leq 20$ km/s) and a high velocity regime ($v > 20$ km/s).

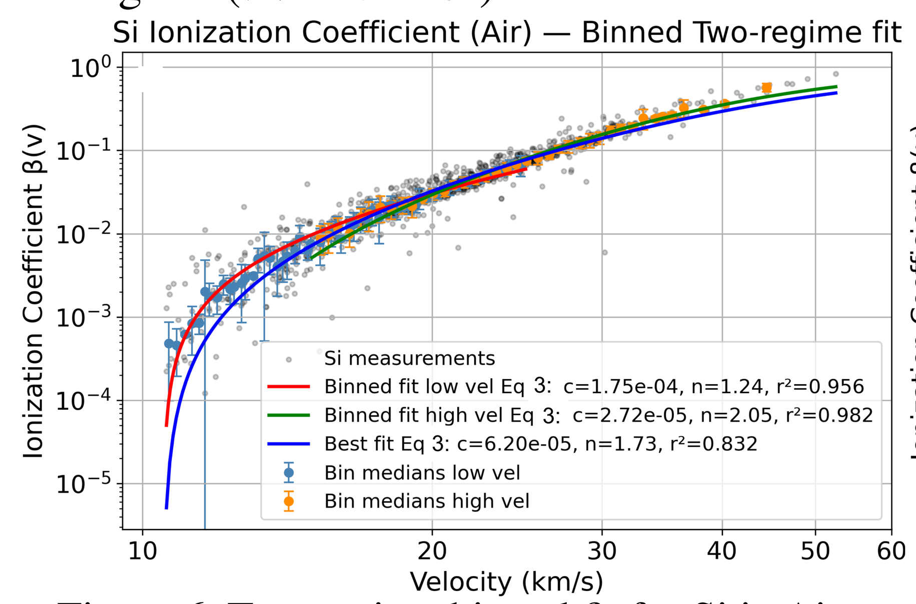

Figure 6. Two regime binned fit for Si in Air.

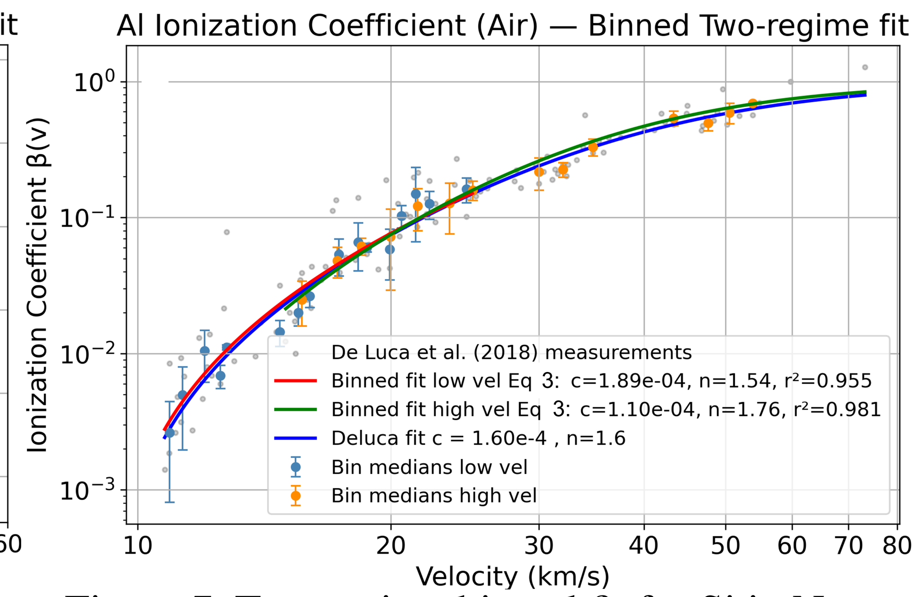

Figure 7. Two regime binned fit for Si in N_2.

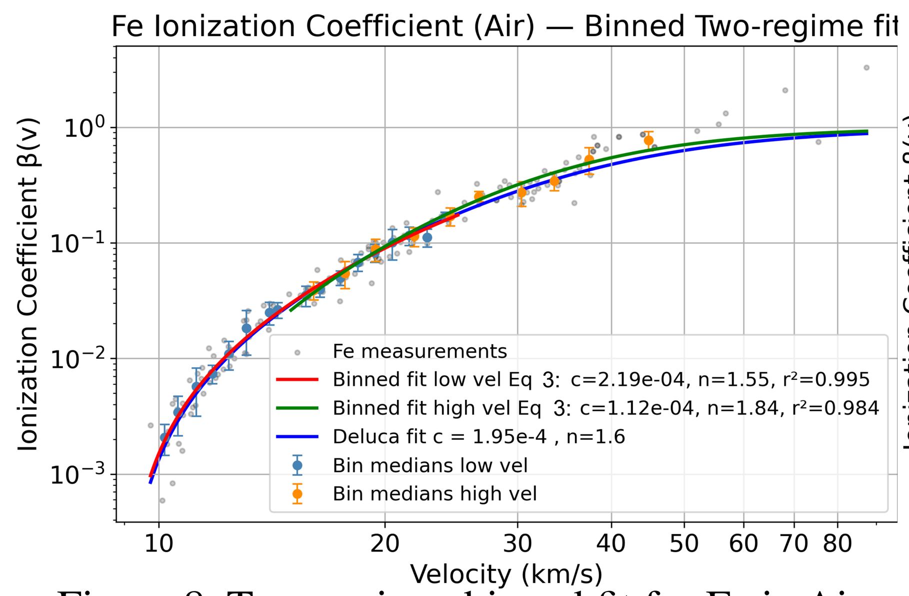

Figure 8. Two-regime binned fit for Fe in Air.

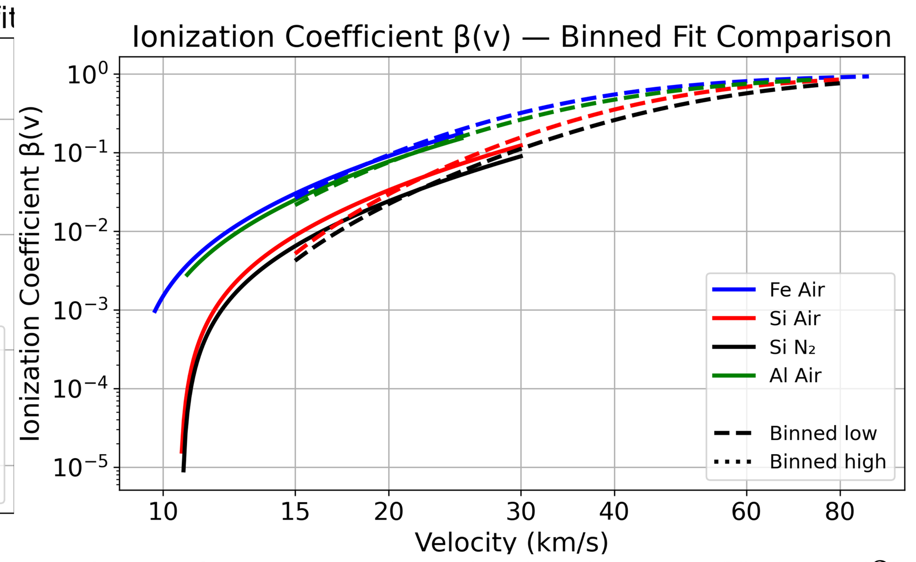

Figure 9. Two-regime ionization coefficient (β) comparison for Fe in air, Si in air, and Si in N2 and Al in Air using Binned Fitting (BF) method.

Table 2. Fitted parameters c and n, and r^2 for the ionization coefficient model (Eq. 3) obtained from the two-regime split approach for Fe and Si in Air and N_2 and Al in Air. The velocity ranges are defined as Low v regime (v ≤ 20 km/s) and High v regime (v > 20 km/s)..

Element	Gas	Regime	c	n	r^2
Fe	Air	Low v	$(2.19 \pm 0.35) \times 10^{-4}$	1.55 ± 0.08	0.995
		High v	$(1.12 \pm 0.53) \times 10^{-4}$	1.84 ± 0.18	0.984
Al	Air	Low v	$(1.89 \pm 0.23) \times 10^{-4}$	1.54 ± 0.03	0.955
		High v	$(1.10 \pm 0.28) \times 10^{-4}$	1.76 ± 0.07	0.981
Si	Air	Low v	$(1.75 \pm 0.05) \times 10^{-4}$	1.24 ± 0.02	0.956
		High v	$(2.72 \pm 0.41) \times 10^{-5}$	2.05 ± 0.05	0.982
Si	N_2	Low v	$(1.28 \pm 0.20) \times 10^{-4}$	1.22 ± 0.08	0.966
		High v	$(2.83 \pm 1.29) \times 10^{-5}$	1.91 ± 0.16	0.930

Conclusions

- New measurements of β_{Si} in Air and N_2 were presented alongside extended velocity range measurements for Fe. β_{Si} was found to be one order of magnitude lower than Fe, with c values lower than previous theoretical estimates and higher in Air than in N_2.
- A two-velocity regime analysis was proposed for low (v ≤ 20 km/s) and high (v > 20 km/s) velocities, improving past model estimates. The parameter n is consistently higher at high velocities across all elements, suggesting rapid ionization increase possibly due to secondary ionization.
- The obtained c and n values can be incorporated into major ablation models such as CABMOD/ELINDEN [1, 4], improving our understanding of meteor ablation and the accuracy of meteor radar detection.

References
[1] Carrillo-Sánchez, J. D., Plane, J. M. C., Janches, D., & Villanueva, G. L. (2024). Accretion of Meteoric Organic Matter at the Surface of Mars and Potential Production of Methane by Ultraviolet Radiation. *The Planetary Science Journal*, *5*(7), 160. https://doi.org/10.3847/PSJ/ad54c9
[2] DeLuca, M., Munsat, T., Thomas, E., & Sternovsky, Z. (2018). The ionization efficiency of aluminum and iron at meteoric velocities. Planetary and Space Science, 156 , 111-116. doi: 10.1016/j.pss.2017.11.003515
[3] Janches, D., Swarnalingam, N., Carrillo-Sanchez, J. D., Gomez-Martin, J. C., Marshall, R., Nesvorny, D., . . . Pokorny, P. (2017). Radar detectability studies of slow and small zodiacal dust cloud particles. iii. the role of sodium and the head echo size on the probability of detection. The Astrophysical Journal , 843 ,1. doi: 10.3847/1538-4357/aa775c
[4] Jones, W. (1997, 7). Theoretical and observational determinations of the ionization coefficient of meteors. Monthly Notices of the Royal Astronomical Society, 288 , 995-1003. doi: 10.1093/mnras/288.4.995
[5] Vondrak, T., Plane, J. M. C., Broadley, S., & Janches, D. (2008). A chemical model of meteoric ablation. Atmospheric Chemistry and Physics, 8 , 7015-7031.599 doi: 10.5194/acp-8-7015-2008

2026 NSF CEDAR Workshop